A Diiron(III,IV) Imido Species Very Active in Nitrene-Transfer Reactions**

Eric Gouré, Frédéric Avenier, Patrick Dubourdeaux, Olivier Sénèque, Florian Albrieux, Colette Lebrun, Martin Clémancey, Pascale Maldivi, and Jean-Marc Latour**

Abstract: *Metal-catalyzed nitrene transfer reactions arouse intense interest as clean and efficient procedures for amine synthesis. Efficient Rh- and Ru-based catalysts exist but Fe alternatives are actively pursued. However, reactive iron imido species can be very short-lived and getting evidence of their occurrence in efficient nitrene-transfer reactions is an important challenge. We recently reported that a diiron(III,II) complex is a very efficient nitrene-transfer catalyst to various substrates. We describe herein how, by combining desorption electrospray ionization mass spectrometry, quantitative chemical quench experiments, and DFT calculations, we obtained conclusive evidence for the occurrence of an {Fe^III Fe^IV= NTosyl} intermediate that is very active in H-abstraction and nitrene-transfer reactions. DFT calculations revealed a strong radical character of the tosyl nitrogen atom in very low-lying electronic configurations of the Fe^IV ion which are likely to confer its high reactivity.*

Metal-catalyzed nitrene-transfer reactions arouse intense interest as clean and efficient procedures for the synthesis of biologically or pharmacologically active amines.[1] Efficient rhodium-based catalysts have been described[2] but intensive efforts are currently devoted to replacing these heavy metals by iron systems.[3] Owing to their close analogy with the now well-established Fe^IV oxo complexes, obtaining reactive Fe^IV imido species has become a major endeavor. Such Fe^IV imido species could be formed by using highly encumbered ligands of low denticity to isolate three- and four-coordinate imido Fe complexes, but these systems until recently did not exhibit a strong reactivity.[4–6] In contrast, five- and six-coordinate Fe imido species mediate efficient nitrene transfers[7–11] and have

proven so far too reactive to be isolated except in a few particular instances.[7,9,10] Metal imido species can indeed be very reactive and extremely short-lived (sub-microsecond) making their probing by usual techniques difficult and their isolation impossible. Thus getting evidence of their occurrence in efficient nitrene-transfer reactions is currently an important challenge.

We have reported that the diiron(III,II) complex **1** (Scheme 1) was very efficient in catalytic nitrene transfers to alkenes and thioanisole.[12] In addition, its unprotected analogue (with hydrogen atoms in place of chlorine on the
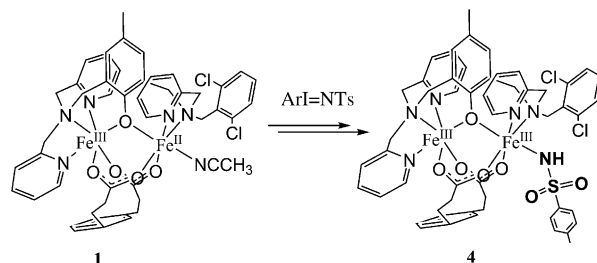
Scheme 1. Reaction of ArI=NTs with the mixed-valent complex **1** with NCCH₃ as a labile ligand [Fe^III Fe^II (NCCH₃)(L-Cl)(mpdp)]²⁺, mpdp = *m*-phenylene dipropionate, Ar = *o*-*tert*-butylsulfonylphenyl, Ts = tosyl, HL-Cl = [2-((bis(pyridyl-2-methyl)amino)methyl][6-((pyridyl-2-methyl)(2,6-dichlorobenzyl))amino)methyl]-4-methylphenol. For simplicity the solvent is not included in the formula.

ortho benzylic positions) was shown to mediate fast and quantitative *ortho*-amination of the dangling benzyl group of the ligand.[13] The remarkable reactivity of these systems prompted us to investigate the nature of the species active in the nitrene transfer to gain information useful to design efficient Fe catalysts for these reactions. Herein we describe how, by using a combination of desorption electrospray ionization mass spectrometry (DESI-MS), quantitative chemical quench experiments, and DFT calculations, we have obtained conclusive evidence for the occurrence of an {Fe^III Fe^IV=NTs} intermediate that is very active in H· abstraction and nitrene-transfer reactions.

When **1** was treated with a tosyl aryliodinane ArI=NTs, the initially blue solution immediately turned red owing to the formation of a new chromophore absorbing at 482 nm.[12] This chromophore was identified as the diferric tosylamido derivative [Fe^III Fe^III (NHTs)(L-Cl)(mpdp)]²⁺ **4** (Scheme 1). As observed in several instances, **4** could originate from an intra- or intermolecular H· abstraction by a higher valent imido intermediate [Fe^III Fe^IV(=NTs)(L-Cl)(mpdp)]²⁺ (**3**).[4,14]

[*] Dr. E. Gouré, Dr. F. Avenier, P. Dubourdeaux, Dr. O. Sénèque, Dr. M. Clémancey, Dr. J.-M. Latour
Université Grenoble Alpes, LCBM, and
CEA, DSV, iRTSV, LCBM, PMB, and
CNRS UMR 5249, LCBM
38054 Grenoble (France)
E-mail: jean-marc.latour@cea.fr

C. Lebrun, Dr. P. Maldivi
Université Grenoble Alpes, UMR E3, and
CEA, DSM, INAC, SCIB, RICC
38054 Grenoble (France)
E-mail: pascale.maldivi@cea.fr

Dr. F. Albrieux
CCSM UMR 5246 CNRS-Université Claude Bernard Lyon 1 (France)

In the hope to detect it, we monitored the formation of **4** by optical stopped-flow spectroscopy in acetonitrile at room temperature. Its formation was evidenced by an absorption growing at 482 nm with a simultaneous decrease of the band at 611 nm and an isosbestic point at 595 nm (Supporting Information, Figure S1). The same spectroscopic features were observed in low-temperature experiments (down to −80 °C) in propionitrile (Figure S2). The 611 nm absorption could be associated with an $Fe^{IV}=NTs$ species since they have been reported to have a low-intensity absorption near 650 nm.[8,9] We thus monitored the reaction by Mössbauer spectroscopy at −80 °C in the hope of trapping **3**. Figure S3 shows the evolution of spectra recorded at times spanning the range 0 to 21 min. These spectra can be explained by the transformation of **1** into another $Fe^{III}Fe^{II}$ species **2** and into **4** but do not uncover an Fe^{IV} derivative. Interestingly, **4** appeared as a mixture of two $Fe^{III}Fe^{III}$ components which differ in the quadrupole splitting (QS) of a single site (Table S2 and see below). These experiments therefore demonstrate that **3** does not accumulate in the millisecond time scale because its rate of formation is smaller than its rate of reaction through H⋅ abstraction. A faster technique was thus needed. Such a situation was successfully addressed very recently by DuBois and co-workers[15] who could detect intermediates in the nitrene-transfer reactions of a dirhodium catalyst using the DESI-MS technique, suited to identifying intermediates with lifetimes shorter than milliseconds.[16,17]

We used this technique to study the reaction of **1** with ArI=NTs or its ^{15}N analogue at room temperature. Compound **1** deposited on a polymer surface, was treated with a solution of ArI=NTs in anhydrous acetonitrile. Apart from the signals of **1** and ArI=NTs at *m/z* 464.0727 and 493.9967, respectively, the experimental mass spectrum (Figure 1) showed patterns of signals for dications at *m/z* values of approximately 549.1 and 710.5655. The signal at 710.5655 is assigned to **2**, the iodinane adduct of **1** [$Fe^{III}Fe^{II}$(ArI=NTs)(L-Cl)(mpdp)]$^{2+}$. This assignment was based on the perfect match with the expected mass, the close similarity of the experimental and theoretical isotopic distribution, and the shift of half a mass unit of the whole pattern when using ArI=^{15}NTs (Figure S6). The isotopic pattern in the range *m/z* 547.5–552.0 is more complicated and does not correspond to a single species. Indeed the observed masses could be associated to a mixture of **4** (*m/z* 549.0850) and the sought after imido intermediate **3** (*m/z* 548.5804). This conclusion is supported by the fact that 1) the isotopic patterns recorded at various times could be reproduced very satisfyingly by mixtures of **3** and **4** with various ratios ranging from 70/30 to 10/90 (Figure S7), 2) when thioanisole, a substrate of the nitrene-transfer reaction, was added to the iodinane reactant solution the isotopic pattern matched that of **4** alone (Figure S8), which is consistent with a fast reaction of **3** with thioanisole competing with H⋅ abstraction, and 3) most importantly, when ArI=^{15}NTs was used the pattern expected for **3-^{15}N** at *m/z* 549.0825 was indeed observed (Figure 1 inset). These DESI-MS experiments thus allows the spectroscopic and reactivity observations to be rationalized in the catalytic cycle shown in
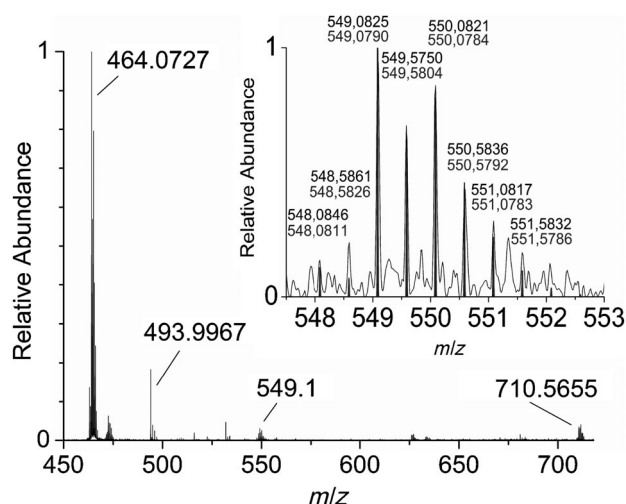

Figure 1. DESI-MS monitoring of the reaction of **1** with ArI=NTs. Inset: superimposition of the experimental (line) and calculated (bars) isotopic patterns of the nitrenyl derivative **3-^{15}N** obtained by reaction with ArI=^{15}NTs.

Scheme 2.[18] Reaction of **1** with ArI=NTs rapidly forms the iodinane adduct **2** detected in the optical (at 611 nm) and Mössbauer low-temperature experiments. Compound **2** decomposes into the imido intermediate **3** that accumulates only to a small extent (detectable solely in DESI-MS experiments) owing to its very high reactivity and either transfers the NTs group to thioanisole to give **5** or abstracts a H⋅ to give the amide **4**.

Chemical quench experiments were then undertaken to further probe and quantitate the formation of **3**. In a typical experiment **1** was treated with ArI=NTs in the presence of a 1-electron or 2-electron donor (2,4-ditertbutylphenol, DTBPH, or thioanisole, Ph-S-Me, respectively). The reaction was monitored by UV/Vis spectroscopy to determine the
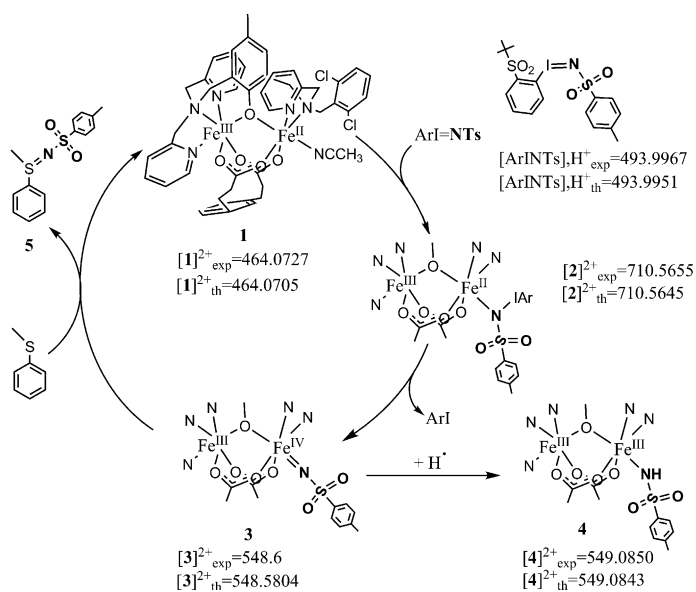
Scheme 2. Cycle accounting for the species identified in the DESI-MS experiments.
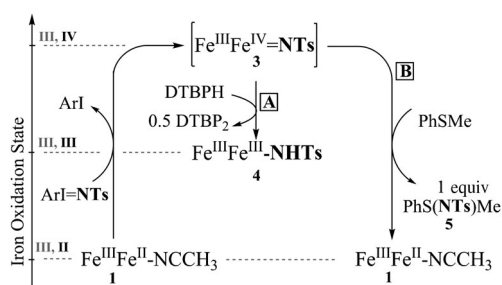
Scheme 3. Experiments used to determine the formation of **3**, see text for details.

oxidation state (Fe^{III}Fe^{II} vs Fe^{III}Fe^{III}) of the resulting complex. The electron count of the reaction was determined by NMR spectroscopy and HPLC quantification of the product/ArI= NTs ratio. These experiments are summarized in Scheme 3. In a first experiment (A in Scheme 3), **1** was treated with 1 equivalent of ArI=NTs in the presence of 1 equivalent of DTBPH. UV/Vis spectroscopy showed the disappearance of **1** and formation of **4** while NMR analysis indicated the formation of 1 equivalent of the dimer (DTBP)$_2$ and therefore the abstraction of a single H· (Figure S9, S10). This result showed that the oxidation state of **3** is one unit higher than that of **4** and that **3** contains an NTs group. In a second experiment (B in Scheme 3), **1** was again treated with 1 equivalent ArI=NTs but this time in the presence of 10 equivalents of Ph-S-Me. The UV/Vis spectrum was unchanged after the reaction and 1 equivalent of sulfilimine **5** Ph-S(NTs)Me was formed (Figure S11, S12). These observations revealed that the oxidation state of **3** is two units higher than that of **1** and that it can transfer an NTs group. All these results suggest that **3** can be formulated as a {Fe^{III}Fe^{IV}(= NTs)} species.

We then intended to characterize the high reactivity of **3** both in nitrene-transfer and H·-abstraction reactions in a more quantitative manner. Owing to the very fast rate of the sulfimidation reaction, we resorted to competition experiments between substituted thioanisoles. In a typical experiment, **1** was treated with 1 equivalent ArI=NTs in the presence of a mixture of 10 equivalents of thioanisole and 10 equivalents of a *para*-substituted thioanisole (*p*-X-Ph-S-Me, X = NO$_2$, COMe, Cl, Me, OMe). The reaction mixture was analyzed by HPLC to quantify the two sulfilimines: Ph-S(NTs)-Me and *p*-X-Ph-S(NTs)-Me. The ratio of the quantities of sulfilimines was taken as the ratio of the kinetic constants of the two reactions. The results are summarized in Table S4. Figure S13 shows that $\log k_X/k_H$ is linearly correlated ($r^2 = 0.97$) to the redox potentials of the thioethers with a slope of $-1.9(2)$. This result indicates that the sulfimidation occurs by a direct nitrene transfer (instead of a one-electron oxidation and recombination).[19] In addition, a linear correlation ($r^2 = 0.98$) of $\log k_X/k_H$ versus the Hammett constant $\sigma_{p+}(X)$ is observed with a slope $-0.74(6)$ revealing the strong electrophilicity of **3** (Figure S14).

The strong H·-abstraction ability of **3** is the cause of its transiency and we searched to assess this ability further. As shown in Scheme 3A, DTBPH acts as an H· donor to produce

4 but the source of the H· atom in absence of DTBPH is unknown. In our conditions, simple consideration of the respective bond dissociation energy (BDE) values suggest that the eight benzylic positions of the ligand HL-Cl and dicarboxylate mpdp^{2-} are the most likely H· donors. This was confirmed by titrating **1** by ArI=NTs in absence and presence of a very good H· donor, dihydroanthracene (DHA, BDE = 76 kcal mol^{-1}) and monitoring the absorbance at 482 nm (Figure S15). In absence of DHA, a plateau was obtained after addition of approximately 0.9 equivalents of ArI=NTs at an absorption of 1.6. In presence of DHA, the plateau was obtained at approximately 1.0 equivalents of ArI=NTs and an absorption of 1.75. The higher value of the plateau in presence of DHA indicates that in its absence part of the chromophore is consumed. The quantitative difference of about 12% is consistent with the presence of eight reactive benzylic positions in the complex that would account for most of the H· for the formation of **4**. In the course of our low-temperature experiments intended to trap **3** we noticed that at -60°C, after an initial time lag (Figure S2), formation of **4** occurred monoexponentially with $t_{1/2} \approx 57$ s. Since **3** does not accumulate in the reaction, its decay by H· abstraction is faster than its formation. Owing to the presence of 16 benzylic hydrogen atoms it can be roughly estimated that at -60°C the rate of H· abstraction is $k^H \gg 1/(t_{1/2})$[complex] $\approx 6 \, \text{M}^{-1} \text{s}^{-1}$. This value is in the range observed for the most reactive compounds described by Sorokin[20] pointing to a very strong H· abstraction capability of **3**.

The experiments have provided evidence for the formation of **3** and shown that it cannot be intercepted and spectroscopically characterized. To investigate its molecular and electronic structures, we thus relied on DFT calculations. Firstly, thanks to the extensive computational literature on Fe complexes, we successfully calibrated our calculations of structural and Mössbauer parameters on related known dinuclear Fe complexes as well as a mononuclear imido Fe^{IV} species (Tables S5–7). Then both bridging and terminal binding modes of the N(H)Ts group were considered. Moreover, because in **1** the solvent binds in the position *trans* to the bridging phenoxide[21,22] whereas in the insertion product of the non-chloroprotected ligand, the N-benzyltosylate is bound in the *cis* position,[13] we considered both *cis* and *trans* isomers for the calculations of **3** and **4**. First, we explored the tosylamido complex {Fe^{III}Fe^{III}-NHTs} **4** and observed that the terminal mode is clearly preferred, the bridging structure being about 23 kcal mol^{-1} higher. The terminal *cis* and *trans* isomers were very close in energy (*cis* 4.2 kcal mol^{-1} lower than *trans* at the B3LYP level). An illustration of the molecular structure and the bond lengths to each iron atom are given in Figure S18 and Table S8. The relevant optimized parameters featuring the Fe^{III}–NHTs bond are in remarkably good agreement with the X-ray structure of the six-coordinate tolylamido Fe^{III} compound described by Borovik et al.[14] with an Fe^{III}–N bond of 1.968 Å and a Fe-N-S angle of 127°, whereas our optimized Fe^{III}–N$_{Ts}$ bond is 1.94 Å, with a Fe-N-S angle of 128°. Compound **4** was isolated in the low-temperature experiments as a mixture of two species differing mostly by their QS values (Figure S3). The values of the Mössbauer QS calculated for the *cis* and *trans* isomers of **4** are in very

good agreement with those observed experimentally for the two species thus allowing to assign their structures (Table S2).

After the validation of our computational procedure for complex **4** we performed the same analysis on the $\{Fe^{III}Fe^{IV}=NTs\}$ intermediate **3** taking into account the two possible spin states for Fe^{IV}, $S=1$ and $S=2$. The bridging mode is found again at higher energies than the terminal one by at least $16\ kcal\,mol^{-1}$, while the *cis* mode proved to be more stable than the *trans* mode by at least $7\ kcal\,mol^{-1}$.

One prominent result of the geometry optimizations is the close energy of both $S=1$ and 2 spin states (difference less than $4\ kcal\,mol^{-1}$ at the B3LYP level). A second major result is the existence of four low-lying configurations arising from N_{Ts}-to-Fe^{IV} charge-transfer states for $S=1$ and $S=2$ which are easily identified by characteristic spin densities (see below and Supporting Information for details). Careful optimizations of the geometries of these different configurations by control of the spin polarizations of Fe and N_{Ts} atoms yielded structural parameters gathered in Tables S10 and S11 while Figure 2 illustrates the structure of **3** in the most stable *cis* mode. The Fe–ligand bond lengths in Tables S10 and S11 are consistent with experimental Fe^{III} or Fe^{IV} bond lengths. Of particular interest is the short $Fe–N_{Ts}$ distance (ca. 1.71 Å) of the iron-imido group in species **3** $S=1$, very close to the corresponding distance found in the complex reported by Que et al. (1.73 Å).[9]
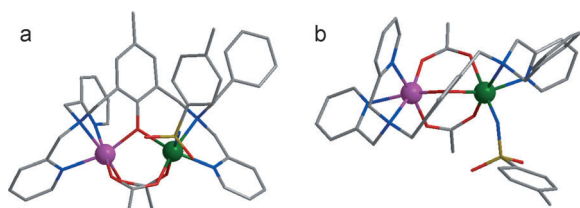

Figure 2. DFT optimized structure of **3**. a) front view, b) top view along the phenoxide main axis magenta Fe^{III}, green Fe^{IV}. Bond lengths and angles are collected in Table S10.

Another remarkable feature emerges from our detailed investigation of the electronic structure of **3** based on spin densities. Indeed, all low-lying configurations have an enhanced radical character of the N_{Ts} donor atom (Table 1 and Table S12). As is usual, we observed a reduced spin

Table 1: Spin densities (ρs) and total bonding energies (eV) computed at the B3LYP level, for complex **3** in *cis* coordination mode.[a]

| | $Fe^{III}_{5/2}$-·N_{Ts} | $Fe^{IV}\ S=2$ | | $Fe^{IV}\ S=1$ |
		Fe^{IV}-βN_{Ts}	Fe^{IV}-αN_{Ts}	$Fe^{III}_{1/2}$-·N_{Ts}
E B3LYP	−774.44	−774.48	−774.63	−774.40
ρs Fe^{IV}	4.03	3.36	4.07	0.94
ρs N	1.1	0.33	−0.40	0.93
ρs O_b	−0.05	−0.13	0.07	−0.16

[a] Spin densities (ρs) of Fe atom, N_{Ts}, and the phenoxide bridging oxygen (noted O_b), and total bonding energies (eV) computed at the B3LYP level. Values are given for the broken symmetry state of **3** ($Fe_2^{III,IV}$ binuclear complex). Configurations noted Fe^{IV}-βN_{Ts} and Fe^{IV}-αN_{Ts} correspond to partial charge transfer configurations (see Supporting Information).

polarization from 5 to about 4 for a high-spin Fe^{III} ion owing to donation from ligands. For Fe^{IV}, spin polarized donation from ligands also occurs, and in particular from the N_{Ts} and O_b (phenoxide) atoms. In the O_b case, the absence of significant radical character on the O_b atom (Table 1) and the presence of six equivalent C−C bonds in the phenoxide ring regardless of the electronic configuration exclude any possibility of a phenoxyl radical (see Supporting Information).

Two configurations arising from the $S=2$ state (Fe^{IV}-αN_{Ts} and Fe^{IV}-βN_{Ts}) exhibit partial radical character on ·N_{Ts}. In contrast, the third configuration ($Fe^{III}_{5/2}$–·N_{Ts}) involves a complete charge transfer resulting in a high-spin Fe^{III} atom bonded to a nitrenyl radical. A complete charge transfer also gives rise to the $Fe^{III}_{1/2}$–·N_{Ts} configuration in the $S=1$ state. Both radical states are consistent with other Fe−N(imido) systems.[4,6,9,23] Note that the optimized geometries corresponding to these two Fe^{III}–·N_{Ts} configurations exhibit $Fe−N_{Ts}$ bonds consistent with Fe^{III} spin state ($S=5/2$ or $1/2$) (see Supporting Information). Such radical character on the nitrogen atom gives rise to a low-energy vacant orbital on this atom. They are represented on Figure 3 for both $S=1$ and $S=2$ states, with their energy level above the SOMO, suggesting in both cases a very high electrophilicity of the N_{Ts} atom.
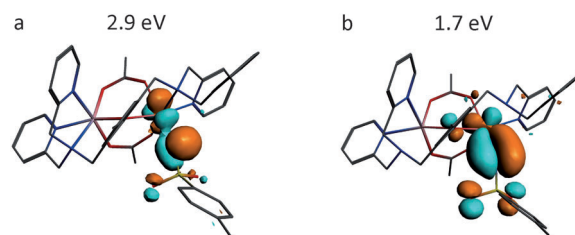

Figure 3. Lowest unoccupied β MO on complex **3** in the a) $S=1$ state; b) $S=2$ state corresponding to the Fe^{III}–·N_{Ts} species (see text), together with its gap above the SOMO at the B3LYP level. Top view from phenoxide axis.

These results are reminiscent of the widely studied Fe^{IV} oxo species derived from heme or non-heme models, known to activate the oxygen-transfer reaction. Their activation mechanism through multiple spin-state pathways has been successfully deciphered by several theoretical and spectroscopic approaches.[24–27] It was also developed for the nitrene-transfer reaction for a heme-model system.[28] In particular, these studies strongly suggest for the $S=2$ pathway, an activated species described as containing a high-spin Fe^{III}–·O moiety.[24,26] In the light of these seminal studies, our finding of Fe^{III}–·N_{Ts} configurations in both $S=1$ and $S=2$ almost isoenergetic states may explain the very high activity of complex **3**.

To summarize, the present study has provided a consistent experimental picture for the occurrence of an $Fe^{III}Fe^{IV}$ imido species **3** formed upon reaction of **1** with the nitrene donor ArI=NTs and its very high reactivity in H·-abstraction and NTs-transfer reactions. This high reactivity that is comparable to the most reactive oxo transfer agents precludes its interception by usual methods responsive to the millisecond

time range. To obtain valuable information on the molecular and electronic structures of **3**, extensive DFT calculations were performed and calibrated on the structures and Mössbauer parameters of several related diiron complexes so as to define a fully reliable methodology. This procedure allowed us to propose for **3** structural parameters (in particular Fe$-$N$_{Ts}$ bond lengths) that are perfectly consistent with those published for similar species. Moreover, it revealed the strong radical character of N$_{Ts}$ in very-low-lying electronic configurations originating from both the S $=$ 1 and S $=$ 2 states of the Fe^{IV} ion that are likely to confer the high reactivity of **3**. Whether this reactivity is associated to the particular environment of the Fe ion or is due to the binuclear nature of the complex is currently being investigated.

[1] G. Dequirez, V. Pons, P. Dauban, *Angew. Chem.* **2012**, *124*, 7498; *Angew. Chem. Int. Ed.* **2012**, *51*, 7384.

[2] J. Roizen, M. Harvey, J. DuBois, *Acc. Chem. Res.* **2012**, *45*, 911.

[3] A. Correa, O. Garcia Mancheno, C. Bolm, *Chem. Soc. Rev.* **2008**, *37*, 1108.

[4] P. L. Holland, *Acc. Chem. Res.* **2008**, *41*, 905.

[5] C. T. Saouma, J. C. Peters, *Coord. Chem. Rev.* **2011**, *255*, 920.

[6] E. R. King, E. T. Hennessy, T. A. Betley, *J. Am. Chem. Soc.* **2011**, *133*, 4917.

[7] J. P. Mahy, P. Battioni, D. Mansuy, J. Fischer, R. Weiss, J. Mispelter, I. Morgenstern-Badarau, P. Gans, *J. Am. Chem. Soc.* **1984**, *106*, 1699.

[8] M. P. Jensen, M. P. Mehn, L. Que, Jr., *Angew. Chem.* **2003**, *115*, 4493; *Angew. Chem. Int. Ed.* **2003**, *42*, 4357.

[9] E. J. Klinker, T. A. Jackson, M. P. Jensen, A. Stubna, G. Juhasz, E. L. Bominaar, E. Münck, L. Que, Jr., *Angew. Chem.* **2006**, *118*, 7554; *Angew. Chem. Int. Ed.* **2006**, *45*, 7394.

[10] P. Leeladee, G. N. L. Jameson, M. A. Siegler, D. Kumar, S. P. de Visser, D. P. Goldberg, *Inorg. Chem.* **2013**, *52*, 4668.

[11] Y. Liu, X. Guan, E. L.-M. Wong, P. Liu, J.-S. Huang, C.-M. Che, *J. Am. Chem. Soc.* **2013**, *135*, 7194.

[12] F. Avenier, J.-M. Latour, *Chem. Commun.* **2004**, 1544.

[13] F. Avenier, E. Gouré, P. Dubourdeaux, O. Sénèque, J.-L. Oddou, J. Pécaut, S. Chardon-Noblat, A. Deronzier, J.-M. Latour, *Angew. Chem.* **2008**, *120*, 727; *Angew. Chem. Int. Ed.* **2008**, *47*, 715.

[14] R. L. Lucas, D. R. Powell, A. S. Borovik, *J. Am. Chem. Soc.* **2005**, *127*, 11596.

[15] R. H. Perry, T. J. Cahill III, J. L. Roizen, J. Du Bois, R. N. Zare, *Proc. Natl. Acad. Sci. USA* **2012**, *109*, 18295.

[16] Z. Takats, J. M. Wiseman, B. Gologan, R. G. Cooks, *Science* **2004**, *306*, 471.

[17] A. B. Costa, R. G. Cooks, *Chem. Phys. Lett.* **2008**, *464*, 1.

[18] DESI normally samples species generated in solution and can be used to identify solution species through MS techniques. However, owing to solvent evaporation the possibility that species detected in DESI conditions are the same as in bulk solution may not be fully warranted. Nevertheless, the strong consistency of our DESI-MS results with those derived from all other bulk solution techniques make this possibility highly unlikely in the present cases.

[19] Y. Goto, T. Matsui, S. Ozaki, Y. Watanabe, S. Fukuzumi, *J. Am. Chem. Soc.* **1999**, *121*, 9497.

[20] E. V. Kudrik, P. Afanasiev, L. X. Alvarez, P. Dubourdeaux, M. Clémancey, J.-M. Latour, G. Blondin, D. Bouchu, F. Albrieux, S. E. Nefedov, A. B. Sorokin, *Nat. Chem.* **2012**, *4*, 1024.

[21] W. Kanda, W. Moneta, M. Bardet, E. Bernard, N. Debaecker, J. Laugier, A. Bousseksou, S. Chardon-Noblat, J.-M. Latour, *Angew. Chem.* **1995**, *107*, 625; *Angew. Chem. Int. Ed. Engl.* **1995**, *34*, 588.

[22] S. Chardon-Noblat, O. Horner, B. Chabut, F. Avenier, N. Debaecker, P. Jones, J. Pécaut, L. Dubois, C. Jeandey, J.-L. Oddou, A. Deronzier, J.-M. Latour, *Inorg. Chem.* **2004**, *43*, 1638.

[23] M. Jaccob, G. Rajaraman, *Dalton Trans.* **2012**, *41*, 10430.

[24] M. Srnec, S. D. Wong, J. England, L. Que, Jr., E. I. Solomon, *Proc. Natl. Acad. Sci. USA* **2012**, *109*, 14326.

[25] S. Shaik, H. Hirao, D. Kumar, *Acc. Chem. Res.* **2007**, *40*, 532.

[26] S. Ye, F. Neese, *Proc. Natl. Acad. Sci. USA* **2011**, *108*, 1228.

[27] S. P. de Visser, J. U. Rohde, Y. M. Lee, J. Cho, W. Nam, *Coord. Chem. Rev.* **2013**, *257*, 381.

[28] Y. Moreau, H. Chen, E. Derat, H. J. Hirao, C. Bolm, S. Shaik, *J. Phys. Chem. B* **2007**, *111*, 10288.